Theoretical Study of the Ground and Excited Singlet States of Styrene†

R. J. Hemley,⊥ U. Dinur,‡ V. Vaida,§ and M. Karplus*

Contribution from the Department of Chemistry, Harvard University, Cambridge, Massachusetts 02138. *Received May 16, 1984*

Abstract: The singlet-state manifold of styrene is examined by use of extended PPP-CI with geometry optimization and CNDO/S-CI techniques. Excitation energies, natural orbitals, equilibrium geometries, and the ethylenic torsional potential of the lower singlet states are determined. The calculated ground-state geometry is in good agreement with experimental results. The effect of double-excitation CI on the excited-state properties is found to be important for the S_3 state, whose excitation energy after geometry optimization is within 0.2 eV of the S_2 state identified in the one-photon absorption spectrum. The S_3 state, in spite of its large double excitation contribution, is calculated to have a significant one-photon oscillator strength. Planar minima are calculated for all four singlet states. In contrast to some earlier analyses, the barrier to rotation about the vinyl bond is found to be significant for the S_1 state. Implications of the excited-state potential surfaces for styrene photoisomerization dynamics are discussed.

I. Introduction

Electronic spectra of aromatic and nonaromatic conjugated molecules have received considerable attention in recent years. Much of the this interest has focused on developing potential energy surfaces to decribe the effects of electronic excitation on nuclear motion. These effects include vibronic spectra and photochemical transformations (e.g., cis-trans isomerization in polyenes). It is useful in this regard to compare the ground- and excited-state potential surfaces of the flexible polyenes[1] with those of the more extensively studied rigid aromatic systems.[2] The molecule styrene is an ideal candidate for such a study because it combines ground- and excited-state features of the vinyl (polyene-like) substituent and of the aromatic phenyl moiety. Thus, it provides a simple system through which we can correlate the general properties of aromatic and nonaromatic π-electron systems. Numerous photochemical studies have been performed on styrene,[3-7] and on a closely related conjugated system, stilbene.[8] In comparison to stilbene, styrene is more tractable for theoretical calculations because of its fewer electrons. This is particularly important in employing methods that go beyond the simple SCF molecular orbital level. Such methods are now known to be necessary to properly treat the full complement of lowest excited (π,π^*) electronic states of conjugated systems.[1]

A detailed picture of the active potential energy surfaces of styrene that is consistent with both the measured spectra and proposed singlet-state photochemistry has not yet emerged.[3-7] The existing problems are exemplified by recent work on the styrene S_1 state. On the basis of interpretations of fluorescence measurements, Hui and Rice[4] proposed that the styrene S_1 state is twisted about the vinyl CH_2 group. In their model, photoexcitation results in a rapid population of a twisted configuration of S_1 which then deactivates to give ground-state cis and trans species. This scheme is supported by the semiempirical calculations of Bruni et al.,[9] who predict that the S_1 and S_2 states, arising from the mixture of the benzene $^1B_{2u}$ state and the ethylene V state, experience an avoided crossing along the CH_2 torsional coordinate to produce a deep nonplanar minimum for S_1. However, this model appears to be inconsistent with analyses of the $S_1 \leftarrow S_0$ transition by Hollas and co-workers[10] and with a recent study of the absorption spectrum measured directly in a free-jet expansion.[12] These $S_1 \leftarrow S_0$ spectra suggest that the S_1 state is planar since they show vibrational development involving primarily ring and substituent-sensitive ring vibrations and do not show any evidence of the CH_2 torsional coordinate progressions expected from the model of Hui and Rice.[4] This interpretation is in agreement with the ab initio CI calculation of Bendazzoli et al.,[11] who find a planar S_1 state with a significant barrier (16 kcal/mol) to isomerization.

In comparison to the first electronic excitations ($S_1 \leftarrow S_0$), the second absorption system is more intense and shows more extended vibrational development. The vibrational structure has been partially resolved by direct absorption in a seeded free-jet expansion.[13] However, the information on this excited state is still incomplete because of the spectral congestion remaining in the main vibrational bands even at the low temperature achieved in the jet ($T_{vib} < 40$ K).[13] Theoretical investigations, including both semiempirical[14-17] and ab initio[11] calculations, predict a strong electronic transition in this region of the spectrum, but there appears to be some disagreement as to its character (variously described as charge transfer,[14,15] delocalized,[16-18] butadienic,[19] and

† Supported in part by grants from the National Science Foundation (CHE-8018318 and CHE-7920433).

⊥ Present address: Geophysical Laboratory, Carnegie Institution, Washington, D.C. 20008.

‡ Present address: Department of Chemistry, Ben-Gurion University of the Negev, Beer Sheva, Israel.

§ A. P. Sloan Fellow, and Camille and Henry Dreyfus Teacher-Scholar. Present address: Department of Chemistry, University of Colorado, Boulder, Colorado 80309.

(1) B. S. Hudson, B. E. Kohler, and K. Schulten, In "Excited States", E. C. Lim, Ed., Vol. 6, Academic, New York, 1982, pp 1-95.

(2) (a) J. B. Birks, "Photophysics of Aromatic Molecules", Wiley, London, 1970. (b) L. D. Ziegler and B. S. Hudson, in "Excited States", E. C. Lim, Ed., Vol, 5, Academic, New York, 1982, pp 41-140.

(3) C. S. Nagakawa and P. Sigal, *J. Chem. Phys.*, **58**, 3529 (1973).

(4) M. H. Hui and S. A. Rice, *J. Chem. Phys.*, **61**, 833 (1974).

(5) (a) H. E. Zimmerman, K. S. Kamm, and D. P. Werthemann, *J. Am. Chem. Soc.*, **96**, 7821 (1974); (b) *Ibid*, **97**, 3718 (1975).

(6) A. L. Lyons, Jr., and N. J. Turro, *J. Am. Chem. Soc.*, **100**, 3177 (1978).

(7) (a) P. M. Crosby and K. Salisbury, *Chem. Soc., Chem. Commun.* **1975**, 477 (1975). (b) R. P. Steer, M. D. Swords, P. M. Crosby, D. Phillips, and K. Salisbury, *Chem. Phys. Lett.*, **43**, 461 (1976). (c) K. P. Ghiggino, D. Phillips, K. Salisbury, and M. D. Swords, *J. Photochem.*, **7**, 141 (1977). (d) K. P. Phillips, K. Hara, G. R. Mant, D. Phillips, K. Salisbury, R. P. Steer, and M. D. Swords, *J. Chem. Soc., Perkin Trans. 2*, **1978**, 88 (1978). (e) K. P. Ghiggino, K. Hara, K. Salisbury, and D. Phillips, *J. Photochem.*, **8**, 267 (1978).

(8) See: (a) J. Saltiel, J. D'Agostino, E. D. Megarity, L. Metts, K. R. Neuberger, M. Wrighton, and D. S. Zafiriou, In "Organic Photochemistry", O. L. Chapman, Ed., Vol. 3, Dekker, New York, 1973, pp 1-113. (b) N. J. Turro, "Modern Molecular Photochemistry", Benjamin, New York, 1978.

(9) M. C. Bruni, F. Momicchioli, I. Baraldi, and J. Langlet, *Chem. Phys. Lett.*, **36**, 484 (1975).

(10) (a) J. M. Hollas, E. Khalilipour, and S. N. Thakkur, *J. Mol. Spectrosc.*, **73**, 240 (1978). (b) J. M. Hollas and T. Ridley, *Chem. Phys. Lett.*, **75**, 94 (1980). (c) J. M. Hollas and T. Ridley, *J. Mol. Spectrosc.*, **89**, 232 (1981). (d) J. M. Hollas, H. Musa, T. Ridley, P. H. Turner, and K. H. Weisenberger, *Ibid.*, **94**, 437 (1982).

(11) G. L. Bendazzoli, G. Orlandi, P. Palmieri, and G. Poggi, *J. Am. Chem. Soc.*, **100**, 392 (1978).

(12) D. G. Leopold, Ph.D. Thesis, Harvard University, 1983.

(13) D. G. Leopold, R. J. Hemley, V. Vaida, and J. L. Roebber, *J. Chem. Phys.*, **75**, 4758 (1981).

(14) H. C. Longuet-Higgins and J. N. Murrell, *Proc. Phys. Soc. London, Ser. A*, **68**, 601 (1955).

0002-7863/85/1507-0836$01.50/0

Table I. Excitation Energies and Oscillator Strengths

transition	excitation energies, eV: CNDO/S-CI[a] vertical	PPP-CI[a] vertical	PPP-CI[b,c] vertical	PPP-CI[c,d] adiabatic	exptl 0–0	oscillator strengths: calcd[a]	calcd[b]	exptl
$S_1 \leftarrow S_0$	4.28	4.51	4.44 (4.61)	4.29 (4.48)	4.31[e]	5.1×10^{-4}	2.9×10^{-4}	2×10^{-3} [g]
$S_2 \leftarrow S_0$	5.40	5.35	5.30 (4.98)	5.01 (4.64)	4.88[f]	0.17	0.16	0.24[h]
$S_3 \leftarrow S_0$	5.92	5.91	5.84 (6.57)	5.19 (6.33)		0.048	0.052	

[a] Initial ground-state geometry. [b] PPP-CI minimized ground-state geometry. [c] Single CI results in parentheses. [d] Energy-minimized geometry used for each electronic state. [e] Reference 10. [f] Reference 13. [g] Reference 12. [h] Reference 15.

ethylenic[11]). Quantitative predictions of the vibrational activity of the spectrum expected for these different types of excitations would be useful in order to assess their accuracy; however, none has been reported.

Interpretation of the second band is further complicated by predictions of a nearby doubly excited electronic transition.[11,18] The electronic and photochemical implications of such low-lying, one-photon forbidden states of doubly excited character have been established in the linear polyenes, where these states are the lowest excited singlets in a number of well-studied cases.[1] The identification of this transition in the spectrum of styrene has not been made. The ab initio calculations[11] find the doubly excited state below the strong, optically allowed transition and give the state a twisted equilibrium geometry. Moreover, the oscillator strength is calculated to be extremely small so that the state does not contribute to the one-photon spectrum. Semiempirical calculations,[18] on the other hand, find that the doubly excited state is slightly above S_2, and in contrast to the ab initio results, these calculations predict that the transition should contribute to the one-photon spectrum.

Understanding the electronic spectrum of styrene is necessary for mapping out the excited-state dynamics of this prototypical system. This in turn requires a characterization of the potential energy surfaces of the electronic states active upon optical excitation. In previous theoretical studies of styrene,[9,11,14-19] the excited-state potential surfaces and their effects on the electronic spectrum were not fully explored. It is important, therefore, to apply to styrene methods that have been used for potential surface calculations on the linear polyenes.[20] A number of detailed predictions concerning measureable spectroscopic quantities have been made for the polyenes; experimental measurements of vibrational frequencies and Franck–Condon factors confirm many of these theoretical results.[21] Similar theoretical calculations of the spectrum of stilbene[22] and other conjugated hydrocarbons[23,24] have also been instructive.

In this paper properties of the singlet states of styrene active in the absorption spectrum are studied by use of extended PPP[20,23] and CNDO/S[25] methods, both of which are implemented with a single and double excitation configuration interaction (CI) basis. Excitation energies, natural orbitals, and oscillator strengths for the ground and lowest singlet states are calculated with special attention given to the effects of energy minimization and double excitation CI. The energy-minimized equilibrium geometries of the lower singlet electronic states are examined and compared with previous experimental[26] and theoretical[27-29] studies of the ground state and with some predictions for the excited states. Finally, the potential surfaces for ethylenic torsion are examined in the rigid and adiabatic rotation limits. In a following paper[30] vibrational modes and Franck–Condon factors determined from the calculated ground and excited potentials are used to calculate spectra which are compared with direct absorption measurements of seeded free-jet expansions of styrene.[12,13]

II. Theoretical Method

The calculations were carried out by use of extended PPP-CI[20,23] and CNDO/S-CI[25] techniques; the two methods, although similar, provide some basis for establishing the validity of the results. The CNDO/S method implemented here is limited to fixed geometries, but it includes all valence electrons at the SCF step and full single and double excitation CI (16 and 136 configurations, respectively) of the π-electrons. The potential energy surfaces are calculated by use of extended PPP-CI. In this method the potential energy as a function of the Cartesian coordinate r for each state M is written

$$V^{M}(r) = V_{\sigma}^{M}(r) + V_{\pi}^{0}(r) + \Delta V_{\pi}^{M}(r)$$

where $V_{\sigma}^{M}(r)$ is an empirical potential energy surface for the σ core of the molecule, $V_{\pi}^{0}(r)$ is the contribution from the π-system to the electronic ground state determined from PPP theory, and $\Delta V_{\pi}^{M}(r)$ is the contribution from single and double excitation CI. The minimum of the total potential is found by a combination of steepest descent and Newton–Raphson minimizations.

Because the potential surface calculations are somewhat time consuming, the PPP calculations were limited to partial double excitation CI (60 configurations), the highest energy configurations being eliminated. Use of the reduced CI basis with 60 double excitations in the extended PPP model to calculate the vertical and adiabatic excitation energies in *trans,trans*-1,3,5,7-octatraene results in the correct state ordering and gives energies to within 0.4 eV of the full single and double CI[20] and complete CI (exact PPP)[31] results. Therefore, the essential properties of the states are expected to be correctly predicted within the double CI model with the truncated basis.

Our implementation of the CNDO/S scheme uses the Ohno[32] parametrization of the repulsion integral, whereas the extended PPP method employs a Nishimoto–Mataga[33] term plus an exponential,[23] the latter being introduced to obtain correct vibrational frequencies in conjugated systems. Previous studies[34,35] of the applicability of different parame-

(15) K. Kimura and S. Nagakura, *Theor. Chim. Acta*, **3**, 164 (1965).
(16) G. W. King and A. A. G. van Putten, *J. Mol. Spectrosc.*, **44**, 286 (1972).
(17) C. J. Seliskar, *J. Phys. Chem.*, **81**, 660 (1977).
(18) I. Baraldi and M. C. Bruni, *Gazz. Chim. Ital.*, **110**, 571 (1980).
(19) G. Buemi, F. Zuccarello, and A. Raudino, *J. Mol. Struct.*, **89**, 43 (1982).
(20) A. C. Lasaga, R. J. Aerni, and M. Karplus, *J. Chem. Phys.*, **73**, 5230 (1980).
(21) (a) R. J. Hemley, J. I. Dawson, and V. Vaida, *J. Chem. Phys.*, **78**, 2915 (1983). (b) B. E. Kohler, T. S. Spiglanin, R. J. Hemley, and M. Karplus, *J. Chem. Phys.*, **80**, 23 (1984). (c) D. G. Leopold, R. Pendley, J. L. Roebber, R. J. Hemley, and V. Vaida, *J. Chem. Phys.*, **81**, 4218 (1984).
(22) A. Warshel, *J. Chem. Phys.*, **62**, 214 (1975).
(23) A. Warshel and M. Karplus, *J. Am. Chem. Soc.*, **94**, 5612 (1972).
(24) A. Warshel and M. Karplus, *J. Am. Chem. Soc.*, **96**, 5677 (1974).
(25) J. Del Bene and H. H. Jaffe, *J. Chem. Phys.*, **48**, 1807 (1969).
(26) (a) W. M. Ralowski, P. J. Mjöberg, and S. O. Ljungren, *J. Mol. Struct.*, **30**, 1 (1976); (b) *Ibid.*, **31**, 169 (1976).
(27) J. Sühnel, K. Gustav, and U. P. Wild, *Z. Chem.*, **17**, 342 (1977).
(28) W. J. Hehre, L. Radom, and J. A. Pople, *J. Am. Chem. Soc.*, **94**, 1496 (1972).
(29) J. E. Almlöf, P. U. Isacsson, P. J. Mjöberg, and W. M. Ralowski, *Chem. Phys. Lett.*, **26**, 215 (1974).
(30) R. J. Hemley, D. G. Leopold, V. Vaida, and M. Karplus, to be published.
(31) I. R. Ducasse, T. E. Miller, and Z. G. Soos, *J. Chem. Phys.*, **76**, 4094 (1982).
(32) K. Ohno, *Theor. Chim. Acta (Berlin)*, **2**, 219 (1964).
(33) (a) K. Nishimoto and N. Mataga, *Z. Phys. Chem.*, **12**, 335 (1957); (b) *Ibid.*, **13**, 140 (1957).
(34) K. Schulten, I. Ohmine, and M. Karplus, *J. Chem. Phys.*, **64**, 4422 (1976).
(35) B. Dick and G. Hohlneicher, *Theor. Chim. Acta (Berlin)*, **53**, 221 (1979).

trizations of the repulsion integral in semiempirical multiple CI calculations of the electronic structure of alternate hydrocarbons suggest that the Ohno formula provides a reasonable approximation for a substituted benzene such as styrene. Comparison of the Ohno and the modified Mataga–Nishimoto formulae as a function of C–C bond length[23] shows that they are similar in the region of chemical bonds, although the Ohno function is slightly steeper. The bond length dependence of the Ohno formula is similar to the parametrization due to Pariser and Parr,[36] which was used in the previous PPP-CI study of the styrene spectrum by Baraldi and Bruni.[18]

III. Results and Discussion

A. Excitation Energies. Table I shows the results of calculations for the transition energies of styrene. The first two columns compare the results of the CNDO/S-CI and extended PPP-CI calculation of the vertical energies by use of a fixed planar ground-state geometry with $r(C_1–C_2)$ = 1.344 Å, $r(C_2–C_3)$ = 1.467 Å, phenyl r(C–C) = 1.397 Å, r(C–H) = 1.080 Å, and all in-plane angles of 120°. This geometry was obtained from microwave studies of para-substituted halostyrenes[26] and has been used in previous calculations. As mentioned above, full single and double excitation CI of the π-electrons is used in the CNDO scheme, whereas a limited double CI basis is employed in the PPP calculation.

In spite of the differences in the calculational methods, the two models predict a similar vertical excitation spectrum. The excitation energies for the three transitions also are close to those calculated by use of a form of PPP-CI with the Pariser–Parr parameterization of the repulsion integral and including triple excitations;[18] previous CNDO-type single CI calculations[16,17] give similar results for $S_1 \leftarrow S_0$ and $S_2 \leftarrow S_0$ but differ significantly for $S_3 \leftarrow S_0$. The important point concerning the double CI results reported here is that the S_3 state is calculated to be well above S_2 in the fixed geometry approximation while the two states are close together if geometry optimization is performed (see below). In a following paper we use the measured absorption spectrum to test the calculated splittings between the excited states.[30]

The excitation energies calculated with geometry optimization preserve the state ordering, but there are important changes in some of the relative energies (see Table I). In performing the minimizations, various starting configurations were chosen with dihedral angles between 0° and 45° for both substituent bonds. In every case, all minimized geometries were found to be planar. Table II gives the calculated geometries, which are discussed in detail below. The PPP-CI excitation energies, including the results of calculations limited to single CI, are listed in columns 3 to 5 of Table I. Only a slight lowering of the PPP-CI vertical excitation energies occurs in going from the idealized to minimized ground-state coordinates. However, the effect of geometry optimization on the excited states is considerable. This is particularly true for the S_3 state. In the double CI calculation, the excitation energy for $S_3 \leftarrow S_0$ drops from 5.84 to 5.19 eV, a stabilization of the excited state relative to the ground state of 0.65 eV; in contrast, the relative stabilization under single CI is 0.25 eV. This difference demonstrates the necessity of including the electron correlation effect introduced by higher CI for a correct description of this type of electronic excitation within a molecular orbital scheme (see below) and for geometry optimization of states with a high degree of correlation. Corresponding results have been found for the 2^1A_g state of the linear polyenes.[20] A smaller effect of energy minimization is calculated for S_1 and S_2; under double CI $S_1 \leftarrow S_0$ drops by 0.14 eV and $S_2 \leftarrow S_0$ by 0.29 eV. As the vibrational development in the electronic spectrum correlates with the change in equilibrium geometry, we expect from these results that the styrene spectrum should show increasing vibronic structure as we proceed from $S_1 \leftarrow S_0$ to $S_3 \leftarrow S_0$.

Finally, the calculated excitation energies, together with the oscillator strengths for the transitions, are compared with those obtained from the measured one-photon absorption spectrum.[10,12,13] As shown in Table I, the calculated excitation energies for $S_1 \leftarrow S_0$ and $S_2 \leftarrow S_0$ are in good agreement with experiment. The calculated oscillator strengths have the correct behavior; i.e., $S_1 \leftarrow S_0$ is very weak while $S_2 \leftarrow S_0$ is much stronger. Quantitatively $S_1 \leftarrow S_0$ is considerably underestimated while $S_2 \leftarrow S_0$ is of the correct order of magnitude. The small splitting of 0.18 eV between the minimized S_2 and S_3 states and the significant oscillator strengths calculated for $S_3 \leftarrow S_0$ suggest that both the S_2 and S_3 transitions may contribute to the second absorption band. The magnitude of the calculated $S_3 \leftarrow S_0$ oscillator strength is in agreement with previous PPP-CI calculations[20] but in disagreement with ab initio results.[11] A detailed examination of the oscillator strengths and transition moments is given below, following a discussion of the properties of the CI wave functions and natural orbitals.

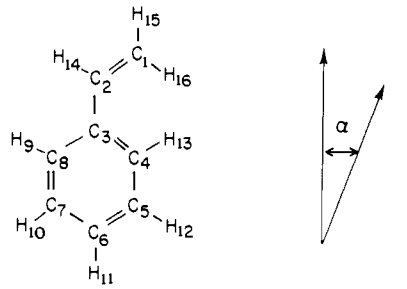

Figure 1. Structure and labeling scheme for styrene.

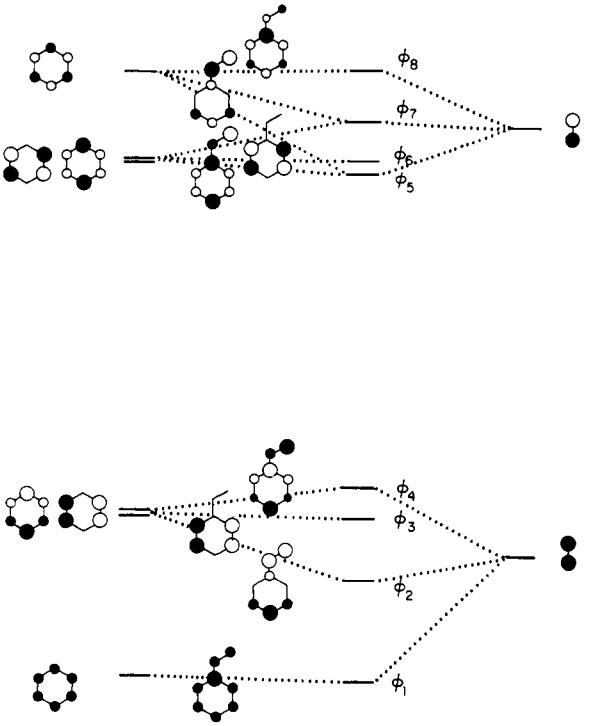

Figure 2. Correlation diagram of the π-orbitals of styrene with those of benzene and ethylene.

B. CI Wave Functions and Natural Orbitals. The CI and geometry optimization effects on the electronic state energies can be understood in more detail by examining the calculated wave functions. Figure 2 gives a correlation diagram of the SCF π-orbitals of styrene, benzene, and ethylene; Table III lists the corresponding LCAO coefficients obtained from the CNDO/S calculation. The principal configurations arising from the full single and double CI which contribute to the ground- and excited-state wave functions are given in Table IV. The SCF orbitals and the leading terms in the CI wave functions are similar to those obtained from the PPP-CI calculation. To further illustrate the CI effects, the natural orbitals[37] are presented in Table V. These were obtained from the CNDO calculation by diag-

(36) P. Pariser and R. G. Parr, *J. Chem. Phys.*, **21**, 767 (1953).

(37) E. B. Wilson and P. S. C. Wang, *Chem. Phys. Lett.*, **15**, 400 (1972).

Table II. Equilibrium Geometries[a]

internal coordinate	electronic state				
	$(S_0)^b$	S_0	S_1	S_2	S_3
	Bond Lengths (Å)				
$r(C_1-C_2)$	(1.344)	1.343	1.381	1.416	1.448
$r(C_2-C_3)$	(1.467)	1.478	1.440	1.405	1.421
$r(C_3-C_4)$	(1.397)	1.417	1.439	1.467	1.469
$r(C_4-C_5)$		1.404	1.436	1.380	1.375
$r(C_5-C_6)$		1.405	1.412	1.431	1.450
$r(C_6-C_7)$		1.405	1.414	1.428	1.444
$r(C_7-C_8)$		1.403	1.436	1.380	1.374
$r(C_8-C_3)$		1.418	1.437	1.470	1.474
$r(C_1-H_{16})$	(1.080)	1.084	1.081	1.079	1.077
$r(C_1-H_{15})$		1.086	1.084	1.082	1.080
$r(C_2-H_{14})$		1.086	1.086	1.085	1.083
$r(C_4-H_{13})$		1.082	1.079	1.080	1.081
$r(C_5-H_{12})$		1.083	1.081	1.083	1.083
$r(C_6-H_{11})$		1.083	1.082	1.081	1.078
$r(C_7-H_{10})$		1.083	1.081	1.084	1.083
$r(C_8-H_9)$		1.083	1.080	1.081	1.082
	In-Plane Angles (deg)				
$\angle C_1C_2C_3$	(120.0)	124.6	124.4	123.7	124.2
$\angle C_2C_3C_4$		122.3	122.4	122.1	122.7
$\angle C_3C_4C_5$		120.3	120.2	119.9	120.5
$\angle C_4C_5C_6$		120.3	120.4	120.7	120.5
$\angle C_5C_6C_7$		119.9	120.3	120.5	119.9
$\angle C_6C_7C_8$		120.1	120.2	120.5	120.4
$\angle C_7C_8C_3$		120.5	120.4	120.1	120.7
$\angle C_8C_3C_2$		118.8	119.0	119.6	119.2
$\angle C_2C_1H_{16}$	(120.0)	122.6	122.3	122.4	121.7
$\angle C_2C_1H_{15}$		119.7	119.3	118.8	118.6
$\angle C_1C_2H_{14}$		119.0	118.1	117.6	117.2
$\angle C_3C_4H_{13}$		120.8	121.1	120.3	119.7
$\angle C_4C_5H_{12}$		119.8	119.4	120.4	120.7
$\angle C_5C_6H_{11}$		120.0	119.9	119.7	120.0
$\angle C_6C_7H_{10}$		119.9	120.2	119.1	118.9
$\angle C_7C_8H_9$		119.6	119.4	120.7	120.6

[a] PPP-double CI calculation. [b] Starting geometry for S_0 energy minimization (from ref 26). All ring r(C–C) = 1.397 Å, r(C–H) = 1.080 Å, and angles = 120.0°.

onalizing the density matrix constructed from the full π-electron CI wave function.

As shown in Table IV, there is only a small contribution from doubly excited configurations to the wave functions of S_0 and S_1. Consequently, the natural orbitals obtained for these two states are similar to the SCF orbitals (comparing Tables III and V). The $S_1 \leftarrow S_0$ transition is dominated by an excitation of half an electron from orbital 3 to orbital 5 and of half an electron from orbital 4 to orbital 6, denoted in Table IV as [3,5] and [4,6], respectively. These two short-axis (B_2 in C_{2v}) excitations resemble those describing the B_{2u} state of benzene.[2] This is in agreement with the ab initio calculations of Bendazzoli et al.[11] (In the ab initio calculation the two leading coefficients of the S_1 wave functions have opposite signs due to different phases used for the SCF orbitals.) Although the state is dominated by these two configurations, the secondary contributions from other configurations are important for the correct description of the polarization of the transition, as discussed in the next section. Bendazzoli et al.[11] state that the double excitations [4 4,5 6], [3 4,5 6], and [3 4,5 5] make significant contributions (but list no coefficients for them); in our study a different set of double excitations (as listed in Table VI) appears to be most important. The discrepancy is most likely related to small differences between the two calculations in the degree of mixing of the ethylenic and benzenic orbitals in the higher virtual MO's.

For the S_2 state, there is significant mixing of ethylenic and benzenic orbitals. The state is dominated by the [4,5] ([HOMO,LUMO]) configuration, which is largely delocalized. Although there are prominent contributions from the substituent orbitals to [4,5], the ring orbitals are important in this configuration as well. The activity of the ring in the S_2 state is further enhanced by the benzenic [3,6] contribution to the CI wave function. The characterization of the S_2 state as delocalized agrees with the results of previous calculations[16-18] but disagrees with others which apparently find the activity to be more localized in the vicinity of the substituent.[11,19] In the ab initio calculation[11] (which involved limited double CI), this state was found to be the third excited singlet, in contrast to the present results.

The large CI effect for the S_3 state gives rise to a complicated excited-state wave function. All significantly occupied natural orbitals are delocalized over the entire molecule so that there are no longer any pure benzene-type orbitals as in the ground state (Table IV). This state has an important contribution from the [4 4,5 5] ([HOMO HOMO,LUMO LUMO]) two-electron excitation, in addition to the primary [4,7] single excitation (Table III). Altogether nine configurations make significant contributions to the excited-state wave function. The S_3 wave function is similar to that obtained in the ab initio calculation.[11] However, the ab initio calculation attributes the largest contribution to the double excitation, and there are differences in the nature of the secondary terms, as discussed in the next section.

C. Oscillator Strengths. A significant test of the quality of the calculation of the excited-state wave functions is the determination of the strength and polarization of transitions between electronic states. In the present case, we focus on the calculation of the one-photon dipole transition moments in the fixed geometry approximation calculated with CNDO/S. Results are obtained for both the intial ground-state and the PPP-CI minimized ground-state geometries (Table I). As mentioned above, fairly good agreement with existing spectra are obtained for the three transitions, particularly if one interprets the second absorption band as containing contributions from both $S_2 \leftarrow S_0$ and $S_3 \leftarrow S_0$. Quantitatively, the $S_1 \leftarrow S_0$ oscillator strength is significantly underestimated in both calculations. Moreover, the polarization of the $S_1 \leftarrow S_0$ transition is calculated to be largely short-axis (B_2) polarization in contrast to the results of rotational band contour analyses[38] which find long-axis (A_1) polarization; this result agrees with previous semiempirical calculations[18] but disagrees with the ab initio results.[11] To analyze these results, we consider the details of the contributions to the transitions.

The [3,5] and [4,6] configurations that contribute to S_1 correlate with the [2,4] and [3,5] configurations of the $^1B_{2u}$ state of benzene.[2] These terms make contributions of opposite sign to the transition moment; in benzene this results in the dipole-forbidden character of the $^1B_{2u} \leftarrow {}^1A_{1g}$ transition. In styrene, the $S_1 \leftarrow S_0$ transition behaves similarly, but the transition moments of the two B_2 excitations do not completely cancel. In addition, according to the present calculation, secondary configurations make some contribution. The leading secondary terms in the CI wave function are also basically B_2 type. The sum of the terms results in a transition with considerable short-axis character, with the transition moment making an angle α of 81° with respect to the C_2–C_3 bond (see Figure 1); α is 83° for the minimized ground state geometry. The difference in magnitude of the oscillator strengths for the two calculations ($f = 5.1 \times 10^{-4}$ and 2.9×10^{-4}) illustrates the dependence of the transition moment on the geometry. With use of the PPP-CI minimized geometry for S_1 (corresponding to the vertical emission spectrum), the oscillator strength is similar to the minimized geometry S_0 result ($f = 2.8 \times 10^{-4}$), but α drops to 65°.

The calculation of the $S_1 \leftarrow S_0$ transition moment also appears to be sensitive to both the level of CI and the parameterization of the semiempirical model. For example, at the single CI level using both Ohno[32] and Nishimoto–Mataga[33] parameterizations of the repulsion integral with CNDO/S, the S_1 state has a contribution from the long-axis polarized [4,5] ([HOMO,LUMO]) excitation which is absent in the double CI calculation. In the Ohno calculation with single CI (initial geometry) the magnitude of the [4,5] coefficient is sufficient to change the overall polarization to $\alpha = 19°$, as S_1 and S_2 essentially invert. The $S_1 \leftarrow S_0$

(38) A. Hartford and J. R. Lombardi, *J. Mol. Spectrosc.*, **35**, 413 (1970).

Table III. SCF π-Orbitals[a]

C_i	ϕ_1	ϕ_2	ϕ_3	ϕ_4	ϕ_5	ϕ_6	ϕ_7	ϕ_8
ϵ_j	−15.788	−12.587	−10.698	−9.842	−0.058	0.495	1.733	3.333
1	0.158	−0.508	−0.004	0.478	−0.473	−0.004	−0.495	0.143
2	0.259	−0.569	0.001	0.316	0.335	−0.001	0.581	−0.245
3	0.463	−0.275	0.007	−0.446	0.450	0.010	−0.294	0.471
4	0.400	0.001	−0.500	−0.311	−0.305	0.492	0.003	−0.396
5	0.358	0.289	−0.500	0.183	−0.184	−0.508	0.284	0.363
6	0.343	0.415	−0.006	0.461	0.456	0.009	−0.408	−0.349
7	0.358	0.294	0.493	0.196	−0.201	0.498	0.290	0.362
8	0.399	0.008	0.506	−0.302	−0.293	−0.501	−0.005	−0.395

[a] CNDO/S-double CI calculation. Orbitals (ϕ_j) are listed in order of increasing energy (ϵ_{jj} in eV's) across the table. The orbital coefficients at each carbon (C_i) are listed in the columns (see Figure 1).

Table IV. CI Wave Functions[a]

S_0	0.96 [0] − 0.12 [3 4,5 6]
S_1	−0.67 [4,6] − 0.59 [3,5] + 0.22 [3,7] − 0.18 [2,6] − 0.11 [3 3,6 8] + 0.10 [3 4,5 8]
S_2	−0.85 [4,5] + 0.45 [3,6] + 0.13 [4,7] + 0.14 [2,7]
S_3	−0.64 [4,7] − 0.50 [4 4,5 5] − 0.26 [2,5] − 0.23 [2 4,5 7] − 0.17 [4,5] − 0.16 [3,6] + 0.15 [4 4,7 7] − 0.13 [2,8] − 0.13 [3 4,6 7] + 0.11 [2 2,5 5]

[a] CNDO/S-double CI calculation. $[i,j]$ and $[i\,j,k\,l]$ are single and double excitation configurations, respectively, where the indices are those of the SCF π-orbitals. 16 single and 136 double excitations were included. Only configurations with coefficients whose magnitude is greater than or equal ot 0.10 are listed.

oscillator strength in this calculation increases to $f = 9.0 \times 10^{-2}$, which is considerably larger than the current experimental estimate ($f = 2 \times 10^{-3}$),[12] and the excitation energies and intensities of the higher transitions are in disagreement with experiment. With Nishimoto–Mataga single CI, the [4,5] term makes a smaller contribution and is insufficient to switch the transition moment to long axis polarization ($\alpha = 66°$). Similar results are obtained by using the PPP approximation instead of CNDO/S.

This analysis suggests that the balance of configurations which yields the correct transition moment for S_1 (e.g., the proper mixing of the [4,5] term) is extremely sensitive to the details of the calculation (geometry, parameterization, extent of CI) and thus beyond the accuracy of the present treatment, although the near forbidden nature of the transition is clearly predicted. The extent to which the model with the current parameterization describes other properties of the S_1 state is explored further in later sections and in the subsequent vibrational analysis of the absorption spectrum.[30]

Table V. Natural Orbitals[a]

C_i	ψ_1	ψ_2	ψ_3	ψ_4	ψ_5	ψ_6	ψ_7	ψ_8
S_0	1.988	1.968	1.952	1.941	0.056	0.048	0.034	0.013
1	0.082	−0.508	0.002	0.495	−0.480	0.005	−0.507	0.058
2	0.178	−0.587	−0.003	0.340	0.345	0.005	0.606	−0.149
3	0.436	−0.344	−0.031	−0.426	0.433	−0.048	−0.362	0.435
4	0.403	−0.038	−0.518	−0.271	0.252	0.520	0.035	−0.399
5	0.385	0.268	−0.481	0.219	−0.232	−0.478	0.258	0.393
6	0.381	0.383	0.033	0.458	0.423	−0.048	−0.357	−0.392
7	0.389	0.233	0.512	0.170	−0.168	0.524	0.208	0.397
8	0.406	−0.070	0.485	−0.318	−0.322	−0.472	0.081	−0.402
S_1	1.950	1.992	1.515	1.416	0.485	0.568	0.065	0.009
1	−0.221	−0.592	0.009	0.343	−0.276	0.003	−0.174	−0.613
2	−0.149	−0.670	0.012	0.133	0.101	−0.013	0.110	0.699
3	0.262	−0.390	−0.015	−0.527	0.542	0.001	0.300	−0.342
4	0.353	−0.157	−0.517	−0.294	−0.316	0.499	−0.369	0.102
5	0.437	−0.026	−0.487	0.250	−0.247	−0.509	0.433	−0.013
6	0.470	0.009	0.016	0.526	0.540	0.001	−0.454	−0.001
7	0.438	−0.027	0.500	0.224	−0.248	0.503	0.440	−0.008
8	0.359	−0.148	0.493	−0.332	−0.323	−0.489	−0.381	0.087
S_2	1.991	1.973	1.792	1.221	0.775	0.207	0.028	0.013
1	0.317	−0.496	−0.045	0.433	−0.325	−0.031	−0.456	0.386
2	0.418	−0.496	−0.008	0.241	0.244	0.005	0.467	−0.493
3	0.476	−0.097	0.069	−0.517	0.521	0.060	−0.028	0.474
4	0.367	0.102	−0.468	−0.363	−0.397	0.469	−0.169	−0.314
5	0.287	0.337	−0.531	0.140	−0.137	−0.540	0.361	0.248
6	0.245	0.467	−0.080	0.449	0.499	0.082	−0.456	−0.225
7	0.292	0.365	0.454	0.276	−0.258	0.457	0.395	0.260
8	0.369	0.150	0.528	−0.242	−0.283	−0.519	−0.224	−0.322
S_3	1.976	1.838	1.936	0.982	0.782	0.074	0.362	0.052
1	0.161	−0.418	0.109	0.374	−0.770	−0.016	0.166	0.161
2	0.247	−0.601	0.178	0.156	0.501	0.042	0.412	−0.314
3	0.457	−0.340	0.134	−0.225	0.174	−0.037	−0.563	0.508
4	0.435	−0.039	−0.459	−0.373	−0.235	0.501	−0.041	−0.390
5	0.406	0.191	−0.530	0.038	0.097	−0.456	0.433	0.333
6	0.363	0.277	−0.052	0.702	0.103	−0.057	−0.422	−0.322
7	0.316	0.436	0.438	0.085	0.063	0.535	0.340	0.324
8	0.344	0.209	0.501	−0.380	−0.213	−0.499	0.047	−0.381

[a] CNDO/S-double CI calculation. The first line listed for each electronic state gives the occupation number for the natural orbitals. The orbital coefficients at each carbon C_i are listed in the following eight lines (see Figure 1).

The higher transitions ($S_2 \leftarrow S_0$ and $S_3 \leftarrow S_0$) are both stronger and essentially long-axis polarized. For the $S_2 \leftarrow S_0$ the magnitude and direction of the transition moment ($f = 0.17$ and $\alpha = 16°$ in the initial ground-state geometry; $f = 0.16$ and $\alpha = 22°$ in the optimized ground-state geometry) are determined almost exclusively by the [4,5] configuration. No experimental data are available for α, but the calculated intensity is in good agreement with the measured spectrum. The transition moment of $S_3 \leftarrow S_0$ ($f = 0.048$ and $\alpha = 18°$; $f = 0.052$ and $\alpha = 19°$) is determined by the single excitation configurations [4,7], [3,6], and [4,5], which make significant dipole contributions. In contrast to the relatively strong $S_3 \leftarrow S_0$ transition found here (and in the previous PPP-CI calculations[18]), the ab initio[11] calculations found that the transition to S_3 (with the large [4 4,5 5] contribution) is significantly weaker. This may be the result of different contributions from the minor configurations in the S_3 wave function (not listed in the ab initio results) and/or differences in the SCF orbitals obtained in the two calculations. The activity of both $S_2 \leftarrow S_0$ and $S_3 \leftarrow S_0$ in the one-photon absorption spectrum is examined in detail in the following paper where band contours calculated from the Franck–Condon factors are used to determine the contributions of each excited state to the spectrum.[30]

D. Equilibrium Geometries. The calculated equilibrium geometries in terms of internal coordinates for the lowest singlet states of styrene are given in Table II. The structure of the ground state itself is of considerable interest, as a complete experimental determination has not yet appeared. The ground-state geometry calculated with single CI is nearly identical with that obtained by Sühnel et al.[27] with use of QCFF/PI; this is not unexpected as the latter is an earlier version of the extended PPP method which is limited to only single CI (and employs a slightly different function for the nonbonded interactions). Upon including double CI the ground state is stabilized with only minor changes in the calculated geometry (e.g., bond length shifts of <0.003 Å). Although the ground-state changes are small, the inclusion of higher CI is important for calculating geometries of the excited states, as discussed below. This is in agreement with the results for polyenes.[20]

Starting with the structure of substituted styrenes obtained from microwave studies,[26] we find that upon geometry optimization the ring–substituent bond length [$r(C_2–C_3)$] increases significantly (from 1.466 to 1.478 Å); in contrast the vinyl bond length [$r(C_1–C_2)$] remains virtually unchanged (1.344 Å vs. 1.343 Å). In the microwave analyses it was assumed that there is no distortion of the ring by the substituent; therefore, the benzene C–C bond lengths were used for the phenyl group. The present calculation vindicates this assumption; however, there is a slight overall expansion of the ring and a small distortion associated with $r(C_3–C_8)$ and $r(C_3–C_4)$, which are ~0.01 Å longer than the other phenyl C–C bonds.

For the substituent, in addition to the increase in $r(C_2–C_3)$, $\angle C_1C_2C_3$ has opened up from the 120° expected from sp^2 hybridization to 124.6°. These changes are a result of steric interaction between the ring and substituent hydrogens (H_{13} and H_{16}; see Figure 1). Structural studies[26] of substituted styrenes in the gas phase based on microwave data have found $\angle C_1C_2C_3$ to be somewhat larger; a recent reanalysis of the data gave an angle of 130°.[10d] These results may imply a larger degree of steric interaction than that calculated here. However, it should be pointed out that part of the unfavorable nonbonded interaction between ring and substituent in the present calculation is relieved by the slight distortion of the ring (i.e., $\angle C_2C_3C_4$ has increased to 122.3° and $\angle C_8C_3C_2$ has decreased to 118.8°). In the analyses of the microwave data, as well as in ab initio calculations of the ground-state geometry,[28,29] no distortion of the ring was allowed. All of these studies agree that in spite of the unfavorable nonbonded interactions, the molecule in the gas phase is planar in the ground state. Nevertheless, it is possible that the molecule may undergo large-amplitude zero-point motion out of plane along the $C_2–C_3$ torsional coordinate as pointed out by Hollas et al.;[10] this would give rise to an averaged structure which is nonplanar. If the potential is very flat for this torsion, it is possible that in the condensed phase intermolecular interactions may have an influence on the planarity of the molecule.

Proceeding now to the excited states, the overall geometry change for excitation to S_1 is relatively small, as expected from the small energy minimization effect on its excitation energy. We calculate an expansion in $r(C_1–C_2)$ from 1.343 to 1.381 Å and a contraction of $r(C_2–C_3)$ from 1.478 to 1.440 Å. These bond length changes are consistent with the leading configurations [3,5] and [4,6] in the S_1 wave function (Figure 2 and Table IV). For the $C_1–C_2$ bond, [3,5] and [4,6] are respectively nonbonding-to-antibonding and bonding-to-nonbonding excitations; for $C_2–C_3$ [3,5] is nonbonding-to-bonding and [4,6] antibonding-to-nonbonding excitations. Thus, a slight expansion of $C_1–C_2$ and a compression of $C_2–C_3$ are expected. There is good agreement between these results and experimental estimates of the bond length changes based on rotational band contour analyses of halostyrenes.[39] This is particularly true for $\Delta r(C_2–C_3)$, with –0.038 (calculated) and –0.04 Å (experimental).[39] For $\Delta r(C_1–C_2)$ the results are +0.038 (calculated) and +0.06 Å (experimental). This discrepancy may be related to the differences noted above between theory and experiment for the polarization of the $S_1 \leftarrow S_0$ transition. For example, increased activity of the [4,5] configuration in the S_1 wave function, in addition to introducing long-axis polarization to the transition, would result in a larger expansion of $C_1–C_2$, as described below.

In addition to shifts in the coordinates of the ethylenic group in the present calculation, the ring has expanded upon excitation to S_1, as in the $^1B_{2u}$ state of benzene. A slight in-plane deformation of the ring is also calculated [$\Delta r(C_4–C_5) = +0.032$ Å and $\Delta r(C_7–C_8) = +0.033$ Å whereas $\Delta r(C_5–C_6) = +0.007$ Å and $r(C_6–C_7) = +0.009$ Å]. In the benzene $^1B_{2u}$ state a symmetrical expansion occurs with $\Delta r(C–C) = +0.034$ Å.[40] From the orbital scheme (Figure 2 and Tables III and IV) this difference between styrene and benzene excited-state geometries is seen to result from the involvement of the [3,7] configuration in the S_1 wave function in styrene (absent in benzene). This term, along with the other leading terms in the S_1 wave function, tends to reduce the bond order in the $C_5–C_6$ and $C_6–C_7$ bonds. However, since the [3,7] configuration has a coefficient of opposite sign from that of the others, it reduces the expected changes and results in only a small shift for these bonds in the excited state. These changes in the ring geometry have important consequences for the excited-state normal modes and Franck–Condon factors.[30]

Considerably larger geometry changes are calculated for the S_2 state. The C–C bond orders and bond lengths have changed significantly throughout the entire molecule. Upon excitation from the ground state $r(C_1–C_2)$ expands to 1.416 Å and $r(C_2–C_3)$ contracts to 1.406 Å. This is not unexpected as the leading configuration in the S_2 wave function ([4,5]) involves a transition which is bonding to antibonding for $C_1–C_2$ and antibonding to bonding for $C_2–C_3$. The ring C–C bonds also show large displacements as a result of the significant activity of orbitals delocalized over the ring. In fact, an appreciable deformation of the ring occurs [i.e., $\Delta r(C_3–C_4) = +0.050$ Å and $\Delta r(C_2–C_3) = +0.052$ Å, whereas $\Delta r(C_4–C_5) = -0.024$ Å, $\Delta r(C_7–C_8) = -0.023$ Å, $\Delta r(C_5–C_6) = +0.027$ Å, and $\Delta r(C_6–C_7) = +0.023$ Å]. Large in-plane angle changes are calculated for S_2 (and S_3) relative to S_1 as a result of the ring deformation. Comparing the displacements for the $1^1B_u \leftarrow 1^1A_g$ transition of the linear polyenes (also the [HOMO,LUMO] transition) calculated by the same method,[20] we find a number of similarities, the most important of which concerns excited-state C–C bond inversion. In 1,3-butadiene, for instance, we calculate changes of $\Delta r(C{=}C) = +0.083$ Å and $\Delta r(C–C) = -0.075$ Å,[20] as compared to $\Delta r(C_1–C_2) = +0.073$ Å and $\Delta r(C_2–C_3) = -0.072$ Å in the styrene substituent bonds. However, in making such a comparison we emphasize that the shifts in the ring coordinates represent an important contribution to the overall displacement of the excited state.

As expected from the previous discussion of the S_3 orbital structure and excitation energies, the largest geometry changes

(39) P. H. Hepburn and J. M. Hollas, *Mol. Phys.*, **26**, 377 (1973).

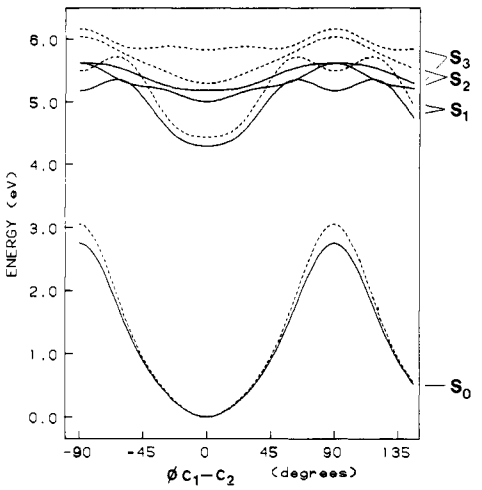

Figure 3. Ethylenic bond torsional potential energy surfaces for styrene in its four lowest singlet states obtained from the PPP-CI model. The dashed lines give the potential energy as a function of rigid rotation with use of the internal coordinates of the energy-minimized geometry of the ground state. The solid lines correspond to adiabatic rotation (full relaxation of the $3N - 7$ remaining degrees of freedom).

Table VI. Ethylenic Bond Torsional Barriers and Local Minima from the PPP-CI Model[a]

state	energy, kcal/mol adiabatic	energy, kcal/mol rigid	angle, deg	
S_0	63.3	70.5	90	barrier
S_1	24.6	29.6	65	barrier
	20.4	24.4	90	minimum
S_2	14.1	17.1	90	barrier
S_3	10.1	7.7	90	barrier

[a] Energy relative to that of the planar configuration with either rigid or adiabatic rotation of the C_1–C_2 bond. The fitted potential curves are given in Figure 3.

are calculated for excitation to this state. There is a large contribution from the [4 4,5 5] two-electron excitation as well as from the [4,7] configuration, both of which introduce considerable antibonding character. Thus, both substituent C–C bonds are somewhat looser in S_3[$r(C_1$–$C_2)$ = 1.448 Å and $r(C_2$–$C_3)$ = 1.421 Å] than in S_2. In addition, the bond alternation in the ring is even more extensive. The magnitude of these geometry changes is similar to those calculated for the $2^1A_g \leftarrow 1^1A_g$ polyene transitions[20] [e.g., in butadiene Δr(C=C) = +0.121 Å and Δr(C–C) = −0.036 Å, as compared to $\Delta r(C_1$–$C_2)$ = +0.105 Å and Δr-$(C_2$–$C_3)$ = −0.057 Å in styrene].

E. Torsional Potentials. The behavior of the potential energy of the molecule as a function of the ethylenic torsional coordinate C_1–C_2 is of central importance for understanding the mechanism of cis–trans photoisomerization. By use of the extended PPP-CI method, the potential energy curves are calculated in two limiting cases. First, the energy in each electronic state is determined as a function of rotation about the C–C bonds with the geometry of ground state used for the remaining internal coordinates (rigid rotation). Second, the energy of each state is calculated at a series of rotation angles while relaxing the other coordinates (adiabatic rotation).[24] Energies were obtained at 0°, 30°, 60°, 80°, and 85°, and the resulting points (including the 180° reflection) were fit with a Fourier expansion; four to six terms were necessary to achieve a good fit without introducing spurious oscillations.

Figure 3 shows the rigid and adiabatic potential energy curves for ethylenic bond torsion in the lower singlet states calculated from the PPP-double CI model. The calculated torsional barriers (in kcal/mol) are listed in Table VI. The adiabatic barrier in the ground state is found to be 63.4 kcal/mol (70.5 kcal/mol for rigid rotation). An experimental determination of this barrier height apparently has not yet been made; however, our result may

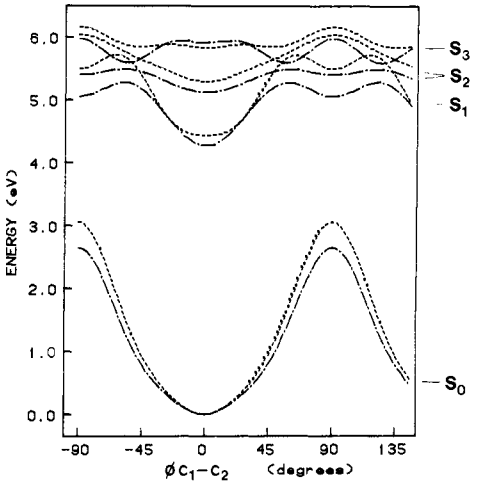

Figure 4. Comparison of the ethylenic bond torsional potentials obtained from the PPP-CI and CNDO/S-CI models (rigid rotation): PPP-CI, dashed line; CNDO/S-CI, dot-dash.

Table VII. Ethylenic Bond Torsional Barriers and Local Minima (kcal/mol) from PPP-CI and CNDO/S-CI Models[a]

state	PPP-CI energy	PPP-CI angle, deg	CNDO/S-CI energy	CNDO/S-CI angle, deg	
S_0	70.5	90	61.1	90	barrier
S_1	29.6	65	22.8	60	barrier
	20.4	90	17.8	90	minimum
S_2	14.1	90	7.4	60	barrier
			5.6	90	minimum
S_3	10.1	90	1.4	90	barrier
			−7.4	60	minimum
			0.7	20	barrier

[a] Energy relative to that of the planar configuration with rigid rotation of the C_1–C_2 bond. The fitted potential curves are given in Figure 4.

be compared to measurements for the ground-state barrier in ethylene (65 kcal/mol)[41] and stilbene (estimated to be 48 kcal/mol).[8] Significantly, upon exciation to S_1 the barrier drops to 24.6 kcal/mol (29.6 kcal/mol rigid) and moves to 65° with a local minimum occurring at 90°. The minimum is 20.4 kcal/mol above the global minimum found for the planar configuration. The local minimum at 90° results from the avoided crossing of the higher states with the S_1 state as the molecule twists. In the higher states the barriers are still smaller; the adiabatic barrier in S_2 is 14.1 kcal/mol (17.1 kcal/mol rigid), and in S_3 it is 10.1 kcal/mol (7.7 kcal rigid).

To understand more fully the dependence of detailed aspects of these results on the particular parameterization of the PPP-CI model, we have also calculated the ethylenic bond torsional potentials with use of CNDO-CI. Since the CNDO/S method is limited to fixed geometries, only rigid bond rotation is considered. The CNDO/S-CI potential curves are plotted in Figure 4, together with the PPP-CI results for rigid bond rotation. From the figure one can see that in the neighborhood of the planar configuration (±30°) the two models give very similar sets of potential curves. (As noted in Table I there is a slight difference in the vertical excitation energies calculated from the two methods.) Upon twisting, the form of the S_0 and S_1 curves are also similar in the two calculations. Table VII further details the comparison between the PPP-CI and CNDO/S-CI results. According to CNDO/S, the barrier for S_1 is 22.8 kcal/mol at 60° (29.6 kcal/mol at 65°

(40) J. R. Lombardi, R. Wallenstein, T. W. Hansch, and D. M. Freidrich, *J. Chem. Phys.*, **65**, 2357 (1976).
(41) J. E. Douglas, B. S. Rabinovitch, and F. S. Looney, *J. Chem. Phys.*, **23**, 315 (1955).

in PPP), and the local minimum is 17.8 kcal/mol above the global minimum at 0° (20.4 kcal/mol in PPP). For the higher states, the differences between the two methods are larger. In S_2 and particularly in S_3, the barriers are much reduced upon going from PPP to CNDO/S, and perhaps more significantly, new minima appear. A local minimum occurs at 90° on the S_2 curve (5.6 kcal/mol above the 0° energy), and a global minimum at 60° develops for S_3 (7.4 kcal below the 0° energy and separated from it by a 0.7-kcal/mol barrier). The latter corresponds to the shallow local minimum for S_3 obtained in the PPP rigid calculation which disappeared in the adiabatic results.

It is useful to compare these results to the ab initio calculation of the torsional potential by Bendazzoli et al.[11] The two studies appear to be in good agreement on the estimate of the rigid barrier height in the ground state (PPP-CI and ab initio both give ~71 kcal/mol). The character of the excited-state torsional potentials is similar in the two studies in that the S_1 and S_2 states (our labeling) are found to be planar, with substantial reductions in the torsional barriers as compared to the ground state. The ab initio calculation predicts a somewhat lower barrier in S_1 (16 kcal/mol) than do our models (~25 and 30 kcal/mol for the two PPP calculations; ~23 kcal/mol for CNDO/S). More significantly, the ab initio and semiempirical calculations disagree both on the question of the local minima for S_1 and on the relative ordering of the excited states (the S_2 and S_3 states are reversed). According to the ab initio calculations, S_3 is nonplanar (as in the CNDO/S results); this results from the contribution from [4 4,5 5] which has a minimum at 90°. In both semiempirical models this configuration becomes the principal term in the S_1 wave function for the twisted molecule. Such an avoided crossing does not appear in the ab initio calculation, perhaps as a result of the limited CI and limited geometry optimization that was employed.

Bruni et al.[9] found that including σ orbitals in their semiempirical CI calculation produces a global minimum at 90° for S_1 separated by a very small barrier from the planar configuration. Using CNDO/S with limited σ–π CI, we obtain potentials which support this result; that is, the twisted configuration for S_1 tends toward a global minimum with a concomitant drop in the barrier height. However, it is difficult to say what level of σ–π CI is appropriate with the standard CNDO/S parameterization (CNDO/2 parameters were used by Bruni et al.), which was established without such CI. Bendazzoli et al.[11] studied the effect of σ–π CI on the torsional potential from an ab initio standpoint and concluded that the effects are small. More important, as pointed out in the introduction, recent spectroscopic studies of the $S_1 \leftarrow S_0$ transition suggest a planar excited state with a sizable barrier. This issue is taken up again in a subsequent paper[30] where the spectrum is analyzed in light of the present theoretical models. We find that the essential features of the S_1 state appear to be well-described assuming σ–π separability with a frozen σ core.

The PPP and CNDO/S torsional potentials calculated in the present treatment predict a substantial barrier to isomarization in the S_1 state; that is, no appreciable cis–trans isomerization will occur in the excited states following excitation of S_1 in the region of its Franck–Condon maximum (the origin). Higher energy excitation of S_1 is required by the present potentials. The nature of the potential curves calculated for the higher singlet states also suggests that they may contribute to photoisomerization. Direct excitation into S_2 and S_3 (which have larger oscillator strengths) followed by rotation on the flatter potential curves for these states would appear to be an efficient excited-state isomerization channel. Because of the relatively larger barrier in S_1, the three excited singlet states are within 5 kcal/mol of each other at 60°; in fact, in the PPP calculation the minimized S_2 curve drops below S_1 at this angle. It is likely, therefore, that as the molecule twists, there is a significant probability of crossing to the S_1 curve and populating the 90° local minimum. Subsequent internal conversion to the ground state would then give partitioning between cis and trans isomers.

This mechanism differs from previous proposals for styrene UV photoisomerization which assumed adiabatic rotation on the S_1 surface alone.[4,9] The present model is more consistent with spectroscopic studies of the $S_1 \leftarrow S_0$ transition,[10] including recent investigations of styrene cooled in a supersonic jet.[12,42] The latter have shown that the vibrational structure of the jet-cooled molecule consists of sharp lines and lacks any sign of C_1–C_2 torsional activity to at least ~1200 cm^{-1} above the origin, indicating that the state is bound for these energies. The model is also consistent with the relatively long fluorescence lifetime (τ_f) of 20 ns reported for the S_1 origin band. Further, the fluorescence quantum yield (φ_f) does not decrease substantially with energy for the main vibronic bands in the spectrum,[42] but there is a dramatic decrease in the region of the $S_2 \leftarrow S_0$ transition under collisionless conditions.[7e] Although this is in accord with the photoisomerization model, other nonradiative processes such as photodissociation at the higher energies cannot be ruled out. It is clear that single vibronic level studies in the high-energy region are necessary to test more fully both the nature of the calculated potential surfaces and the proposed photoisomerization dynamics.

Finally, we compare these results for styrene with studies of the torsional potential surfaces and photoisomerization of its close relative stilbene.[8,43-45] The value of τ_f at the origin of the $S_1 \leftarrow S_0$ ($^1B_u \leftarrow {}^1A_g$) transition of jet-cooled stilbene has been reported to be 2.7 ns, considerably shorter than that of styrene; moreover, it appears to drop off suddenly at ~1200 cm^{-1} excess vibrational energy.[43a] Both spectroscopic studies[44] and theoretical calculations (employing extended CI)[45] indicate that the doubly excited ^1A_g state (analogous to the S_3 state in styrene) lies well above the singly excited ^1B_u state in the planar ground-state configuration. According to the calculations,[45] however, a crossing of the ^1A_g and ^1B_u excited states occurs as a function of the central bond torsion resulting in a global minimum for the ^1A_g state at 90°. Recent spectroscopic results for jet-cooled stilbene have been interpreted in terms of an avoided crossing of these (and possibly other) states.[43] In styrene we find an avoided crossing situation involving three electronic states, with low torsional barriers calculated for S_2 and S_3 (relative to S_0 and S_1) and a 90° minimum for S_1. In styrene the 90° minimum is above the planar minimum of the S_1 curve, and the avoided crossings occur well above (20–30 kcal/mol) the $S_1 \leftarrow S_0$ origin. A similar interaction of the ^1B_u and ^1A_g excited states in 1,3-butadiene has been proposed on the basis of semiempirical calculations (PPP-CI and CNDO/S-CI) of the absorption spectrum,[46] a scheme which is supported by ab initio CI calculations of the double bond torsional potentials.[47]

IV. Conclusion

We have calculated a number of properties of the potential surfaces of the low-lying singlet electronic states of styrene. The orbital structure and equilibrium geometry of the S_1 state largely resembles that of the $^1B_{2u}$ of benzene, although it shows distinct displacements in both the ring and the substituent due to the activity of the substituent orbitals in the $S_1 \leftarrow S_0$ transition. The leading configuration of the S_2 state is the single excitation [HOMO,LUMO] transition. The S_2 geometry is characterized by a considerable deformation of the phenyl ring as well as C–C bond inversion in the substituent. The S_3 state has a large contribution from the [HOMO HOMO,LUMO LUMO] double excitation similar to that calculated for the 2^1A_g states of the linear polyenes. Like the polyene 2^1A_g state, the equilibrium geometry

(42) J. A. Syage, F. Al Adel, and A. H. Zewail, *Chem. Phys. Lett.*, **103**, 15 (1983).
(43) (a) J. A. Syage, W. R. Lambert, P. M. Felker, A. H. Zewail, and R. M. Hochstrasser, *Chem. Phys. Lett.*, **88**, 266 (1982); (b) A. Amirav and J. Jortner, *Ibid.*, **95**, 295 (1983); (c) T. S. Zwier, E. Carrasquillo, and D. H. Levy, *J. Chem. Phys.*, **78**, 5493 (1983).
(44) (a) T. M. Stachelek, T. A. Pazoha, W. M. McClain, and R. P. Drucker, *J. Chem Phys.*, **66**, 4540 (1977); (b) K. Fuke, S. Sakamoto, M. Ueda, and M. Itoh, *Chem. Phys. Lett.*, 74, 546 (1980).
(45) (a) G. Orlandi and W. Siebrand, *Chem. Phys. Lett.*, **30**, 352 (1975); (b) P. Tavan and K. Schulten, *Ibid.* **56**, 200 (1978); (c) G. Orlandi, P. Palmieri, and G. Poggi, *J. Am. Chem. Soc.*, **101**, 3492 (1979).
(46) U. Dinur, R. J. Hemley, and M. Karplus, *J. Phys. Chem.*, **87**, 924 (1983).
(47) V. Bonačič-Koutecký and M. Persico, *Int. J. Quantum Chem.*, **23**, 517 (1983).

of the S_3 state is greatly displaced from that of the ground state. The $S_3 \leftarrow S_0$ transition is calculated to be relatively intense and to be within 0.2 eV of $S_2 \leftarrow S_0$. The height of the calculated ethylenic torsional barrier for S_1 suggests that photoisomerization will not occur in the S_1 state without a large degree of excess vibrational energy. At such energies direct excitation of the higher states (S_2 and S_3), which have larger absorption cross-sections, may in fact be responsible for excited-state cis-trans isomerization.

Acknowledgment. We thank Drs. Bernard Brooks, Doreen Leopold, and Pasquale Tomasello for many useful discussions. We are also grateful to Marilyn Jacobs for her skillful typing of the manuscript.

Registry No. Styrene, 100-42-5.

Dependence of CC and CH Bond Activation on d Band Position: Acetylene on Pt(111) and Fe(100). An Electrochemical Model

S. P. Mehandru and Alfred B. Anderson*

Contribution from the Chemistry Department, Case Western Reserve University, Cleveland, Ohio 44106. *Received January 20, 1984*

Abstract: A study is made of the dependence of CC and CH bond activation energies in acetylene on d band positions when bonded to cluster models of Pt(111) and Fe(100) surfaces. In their normal positions, these bands lie in energy between the acetylene-filled π and empty π^* orbitals. On shifting down (anodic), acetylene π donation to the metals increases and acetylene adsorption energies increase while CC and CH bond scission barriers decrease. On shifting up (cathodic), metal donation to acetylene orbitals increases, also leading to increased acetylene adsorption energies and increased CC and CH activation toward scission. The CC and CH σ and σ^* orbitals also play a role in stabilizing the bond scission transition states. These results, based on atom superposition and electron delocalization molecular orbital theory, are used as a basis for discussing experimental electrochemical work from the literature.

Introduction

In recent studies we have identified a structure effect which determines favored binding sites and influences the distortions of acetylene chemisorbed on (111), (110), and (100) surfaces of iron[1] and platinum.[2] In essence, the carbon atoms in acetylene form as many strong bonds to as many surface metal atoms as possible. When the metal atoms are relatively far apart, as at the 4-fold site of Fe(100) (Figure 1), the adsorbed acetylene molecule is strongly distorted, with a large CC stretch and a large bending of the CH bonds away from the surface. Furthermore, the CC bond is highly activated toward dissociation, which is confirmed by the observed dissociation of acetylene on Fe(100) at 98 K.[3] By contrast, on Pt(111) the metal atoms in the favored triangular site (Figure 1) are relatively close together and the distortions and activation of an adsorbed acetylene molecule are predicted to be less, which is in agreement with experiment.[4] It is of interest to explore the effects of other physical variables in metal surfaces on acetylene adsorption. One such variable is d orbital size. The spacial extents of Fe 3d and Pt 5d orbitals are similar, so an examination of acetylene adsorption on metals with large d orbitals, such as titanium, and small d orbitals, such as copper, would elucidate the importance of carbon p-metal d overlaps. This will not be treated in the present work but is reserved for future studies.[5] Another variable is the metal d band occupation. Again, an explicit study will be reserved for the future, though it may be noted that the orbitals involved in the metal-acetylene bond lie beneath the d band in the iron and platinum examples we have already treated. That is, major acetylene-to-metal π donation and metal-to-π^* back-donation orbitals that are occupied have energies near the bottom or beneath the d band. The major acetylene π plus metal antibonding counterparts lie above the d band and are empty. Thus, d electron count may be a relatively unimportant variable for acetylene adsorption. The final variable to consider is the metal atom d electron ionization potential, that is, the d band position. This is the variable treated in the present study. It is expected that as the d band moves down in energy, acetylene π donation to the metal will increase and metal back-donation to the acetylene π^* orbitals will decrease. What will be the effects of d band position on acetylene geometry and CC bond activation? This study attempts to answer this question in the case of acetylene on Fe(100) and Pt(111) surfaces. In addition, we examine the influence of d band position on CH bond activation. These two surfaces are chosen because acetylene is known to dissociate on clean Fe(100) at monolayer coverage in high vacuum at only 98 K, covering the surface with CH fragments.[3] On Pt(111), the acetylene molecule is stable up to <350 K, and at higher temperature it rearranges and may become hydrogenated.[4]

Our recent studies[1,2a] of acetylene adsorption on the Fe and Pt(111), -(110), and -(100) surfaces show that in each case acetylene π orbitals give rise to bands on adsorption. In the case of the iron surfaces, the π orbital energy levels are stabilized by π donation to the metal d orbitals and are shifted to a position $\sim$1 eV beneath the bottom of the Fe s-d band for Fe_5 and Fe_{21} clusters modeling the (100) surface.[1] This position of the π band relative to the Fe band is in close agreement with photoemission studies.[3] For Pt(111), we have found[2a] a similar π stabilization on adsorption, but in this case the π band is merged into the bottom of the Pt s-d band. This also is in agreement with the results of photoemission studies.[6] On this basis it is reasonable to assume

(1) Anderson, A. B.; Mehandru, S. P. *Surf. Sci.* **1984**, *136*, 398.
(2) (a) Mehandru, S. P.; Anderson, A. B. *Appl. Surf. Sci.* in press. (b) Anderson, A. B.; Hubbard, A. T. *Surf. Sci.* **1980**, *99*, 384.
(3) Rhodin, T. N.; Brucker, C. F.; Anderson, A. B. *J. Phys. Chem.* **1978**, *82*, 894.
(4) (a) Demuth, J. E. *Surf. Sci.* **1979**, *80*, 367. (b) Ibach, H.; Lehwald, S. *J. Vacuum Sci. Technol.* **1978**, *15*, 407. (c) Kesmodel, L. L.; Dubois, L. H.; Somorjai, G. A. *J. Chem. Phys.* **1979**, *70*, 2180.
(5) Work in progress shows acetylene dissociated with no activation energy on all sites of V(100).

0002-7863/85/1507-0844$01.50/0